AFRL-RZ-WP-TP-2008-2114

REATTACHMENT OF A SEPARATED BOUNDARY LAYER ON A FLAT PLATE IN A HIGHLY ADVERSE PRESSURE GRADIENT USING A PLASMA ACTUATOR (POSTPRINT)

Issac G. Boxx, Richard B. Rivir, Jeffery M. Newcamp, and Nathan M. Woods

Turbine Branch
Turbine Engine Division

JUNE 2006

Approved for public release; distribution unlimited.

See additional restrictions described on inside pages

STINFO COPY

AIR FORCE RESEARCH LABORATORY
PROPULSION DIRECTORATE
WRIGHT-PATTERSON AIR FORCE BASE, OH 45433-7251
AIR FORCE MATERIEL COMMAND
UNITED STATES AIR FORCE

REPORT DOCUMENTATION PAGE

Form Approved
OMB No. 0704-0188

The public reporting burden for this collection of information is estimated to average 1 hour per response, including the time for reviewing instructions, searching existing data sources, searching existing data sources, gathering and maintaining the data needed, and completing and reviewing the collection of information. Send comments regarding this burden estimate or any other aspect of this collection of information, including suggestions for reducing this burden, to Department of Defense, Washington Headquarters Services, Directorate for Information Operations and Reports (0704-0188), 1215 Jefferson Davis Highway, Suite 1204, Arlington, VA 22202-4302. Respondents should be aware that notwithstanding any other provision of law, no person shall be subject to any penalty for failing to comply with a collection of information if it does not display a currently valid OMB control number. **PLEASE DO NOT RETURN YOUR FORM TO THE ABOVE ADDRESS**.

1. REPORT DATE *(DD-MM-YY)*	2. REPORT TYPE	3. DATES COVERED *(From - To)*
June 2006	Conference Paper Postprint	01 January 2005 – 01 June 2006

4. TITLE AND SUBTITLE

REATTACHMENT OF A SEPARATED BOUNDARY LAYER ON A FLAT PLATE IN A HIGHLY ADVERSE PRESSURE GRADIENT USING A PLASMA ACTUATOR (POSTPRINT)

5a. CONTRACT NUMBER
In-house

5b. GRANT NUMBER

5c. PROGRAM ELEMENT NUMBER
61102F

6. AUTHOR(S)

Issac G. Boxx and Richard B. Rivir (RZTT)
Jeffery M. Newcamp (Robins Air Force Base)
Nathan M. Woods (Wright State University)

5d. PROJECT NUMBER
2307

5e. TASK NUMBER
06

5f. WORK UNIT NUMBER
2307S314

7. PERFORMING ORGANIZATION NAME(S) AND ADDRESS(ES)

Turbine Branch (AFRL/RZTT)
Turbine Engine Division
Air Force Research Laboratory, Propulsion Directorate
Wright-Patterson Air Force Base, OH 45433-7251
Air Force Materiel Command, United States Air Force

United States Air Force
Robins Air Force Base, GA 31098

Wright State University
Dayton, OH 45354

8. PERFORMING ORGANIZATION REPORT NUMBER
AFRL-RZ-WP-TP-2008-2114

9. SPONSORING/MONITORING AGENCY NAME(S) AND ADDRESS(ES)

Air Force Research Laboratory
Propulsion Directorate
Wright-Patterson Air Force Base, OH 45433-7251
Air Force Materiel Command
United States Air Force

10. SPONSORING/MONITORING AGENCY ACRONYM(S)
AFRL/RZTT

11. SPONSORING/MONITORING AGENCY REPORT NUMBER(S)
AFRL-RZ-WP-TP-2008-2114

12. DISTRIBUTION/AVAILABILITY STATEMENT
Approved for public release; distribution unlimited.

13. SUPPLEMENTARY NOTES
Conference paper published in the Proceedings of the 3rd AIAA Flow Control Conference, June 5 - 8, 2006, in San Francisco, California. Technical paper contains color. PAO Case Number: AFRL/WS 06-1235, 10 May 2006.

The U.S. Government is joint author of this work and has the right to use, modify, reproduce, release, perform, display, or disclose the work.

14. ABSTRACT
An experimental study was performed to examine the phase-dependent response characteristics of a dielectric barrier discharge plasma flow control actuator. The actuator was investigated on a fully separated flat plate boundary layer with an adverse freestream pressure gradient distribution. The actuator was positioned downstream of the boundary layer separation. Phase-locked particle image velocimetry (PIV) was used to obtain two-dimensional velocity field measurements at thirty equally spaced phase-angles along the sinusoidal voltage input to the actuator. A subtle phase-dependence was observed in the response of the streamwise (U-velocity) component of boundary layer velocity field. No similar phase-dependence was observed in the vertical direction (V-component of velocity).

15. SUBJECT TERMS
Plasma control, Dielectric Barrier Discharge

16. SECURITY CLASSIFICATION OF:			17. LIMITATION OF ABSTRACT:	18. NUMBER OF PAGES	19a. NAME OF RESPONSIBLE PERSON (Monitor)
a. REPORT Unclassified	**b. ABSTRACT** Unclassified	**c. THIS PAGE** Unclassified	SAR	16	Rolf Sondergaard **19b. TELEPHONE NUMBER** *(Include Area Code)* N/A

Standard Form 298 (Rev. 8-98)
Prescribed by ANSI Std. Z39-18

Reattachment of a Separated Boundary Layer on a Flat Plate in a Highly Adverse Pressure Gradient Using a Plasma Actuator

Isaac G. Boxx[*] and Richard B. Rivir[†]
Air Force Research Laboratory, Wright Patterson AFB, OH, 45433, USA

Jeffery M. Newcamp [‡]
United States Air Force, Robins AFB, GA, 31098, USA

and

Nathan M. Woods[§]
Wright State University, Dayton, Ohio 45354, USA

An experimental study was performed to examine the phase-dependent response characteristics of a dielectric barrier discharge plasma flow control actuator. The actuator was investigated on a fully separated flat plate boundary layer with an adverse freestream pressure gradient distribution. The actuator was positioned downstream of the boundary layer separation. Phase-locked particle image velocimetry (PIV) was used to obtain two-dimensional velocity field measurements at thirty equally spaced phase-angles along the sinusoidal voltage input to the actuator. A subtle phase-dependence was observed in the response of the streamwise (U-velocity) component of boundary layer velocity field. No similar phase-dependence was observed in the vertical direction (V-component of velocity).

Nomenclature

ρ	=	Freestream air density (kg/m^3)
c	=	Blade Chord Length (m)
C_p	=	$(P_t - P_s)/(1/2\ \rho \mathrm{u}^2)$
P_s	=	Local static pressure (N/m^2)
P_t	=	Total pressure (N/m^2)
Re_c	=	$\rho U_{\mathrm{inf}} c/\mu$
Tu	=	$\sqrt{u'^2 + v'^2}\big/\sqrt{U^2 + V^2}$
U	=	Local Streamwise Velocity (m/s)
U_{inf}	=	Freestream Velocity at Infinity (m/s)
V	=	Local freestream vertical velocity (m/s)
V_{inf}	=	Freestream vertical velocity at infinity (m/s)

I. Introduction

THE increasing demands for greater performance and efficiency in low-pressure turbine blades has lead to higher and higher airfoil loading. A limiting parameter for blade loading is the increased level of boundary layer

[*] NRC Research Associate, AFRL/PRTT, 1950 Fifth St, Wright-Patterson AFB, OH 45423, AIAA Member.
[†] AFRL Fellow, Propulsion Directorate, 1950 Fifth St, Wright-Patterson AFB, OH 45423, AIAA Fellow.
[‡] USAF, Robins AFB, GA 31098, AIAA Member.
[§] Graduate Research Assistant, Department of Mechanical Engineering, AIAA Member.

separation at low Reynolds numbers. In an effort to maintain high blade loading, forestall flow-separation or reattach already separated flows over the LPT at low-Reynolds numbers, various passive and active flow-control mechanisms have been investigated.

Plasma excitation of the wall region offers a method of manipulating the near-wall velocity profile and to induce boundary layer reattachment. The effects of electrostatic fields on fluid flows have been demonstrated over many years. Velkolf (1962) investigated electric field effects on heat transfer and pressure distributions for stagnation and flat plate boundary layer flows. Roth *et al*. (1998) found that a dielectric barrier discharge (DBD) with an asymmetric electrode configuration mounted on a flat plate could reduce drag and also the overall boundary layer thickness by inducing local acceleration of fluid near the wall. Since then, a number of researchers have characterized the effect of these actuators on flow over aerodynamic surfaces. Corke et al. (1997) studied flush mounted and subsurface plasma actuators as a means to introduce controlled disturbances into flow over axisymmetric bodies in supersonic flows of Mach numbers 3.5 and 6. Post *et al.* (2003) studied plasma actuators as a means of controlling flow separation over a NACA 66_3-018 airfoil over Reynolds numbers ranging from 77,000 to 460,000. They demonstrated an 8 degree increase in maximum angle of attack, accompanied by a full pressure recovery after stall. Post *et al.* (2004) also studied the effect of plasma actuators on an oscillating NACA-0015 airfoil and were able to achieve a higher cycle-integrated lift.

Several investigations of the application of the DBD actuators to separated low-pressure turbine (LPT) cascade flows have been reported. Hultgren *et al.*, (2003) studied an array of asymmetric electrode DBD plasma actuators mounted on a flat plat in a simulated pressure field of the suction side of a Pak-B LPT blade at Reynolds numbers ranging from 50,000 to 300,000.   They concluded their phased array DBD plasma actuator was an effective device for separation control on the LPT blade. List *et al.* (2003) studied an asymmetric electrode DBD plasma actuator on a linear cascade of Langston turbine blades and found the actuators could reduce profile loss by 14% at low Reynolds numbers (Re = 30,000).   Huang *et al.* (2003) studied plasma actuators positioned at various chord locations on the surface of a Pak-B profile in a linear turbine cascade over Reynolds numbers ranging from Re_c = 10,000 to 100,000. They found the boundary layer flow reattachment point induced by the plasma actuator was highly sensitive to freestream turbulence and Reynolds number.

Although the studies above have produced useful insight into the effect of plasma actuators on a variety of boundary layer flows, they have relied almost entirely upon time-averaged measurements. While such measurements are useful in studying global effects and trends they also inevitably obscure the periodic nature of the physical mechanism through which these actuators force the near-wall boundary layer flow. Time-averaged measurements are particularly poor in determining what (if any) phase of the actuator cycle is dominant in affecting change in local and global flowfield characteristics. For example, it has been noted by previous researchers (Rivir *et al.*, 2004, Enloe *et al.*, 2004, Orlov *et al.*, 2005) that clusters of very short duration ($\approx$ 10s of *ns*) current spikes form during the ignition phase of the DBD actuator cycle. Peak current during these events can be several orders of magnitude higher than the peak-to-peak current variation elsewhere in the cycle. Figure 1 shows a characteristic voltage and current trace measured in this study. A better understanding of what effect these local current spikes have on the forcing effectiveness of the actuator may be useful in future efforts to optimize these devices for specific flow-control applications.

The objective of the current study was to determine what if any phase-relation exists between the sinusoidal input signal of a DBD actuator and the response of the flow over the actuator. This was accomplished through the acquisition of a statistically meaningful set of phase-averaged velocity field measurements over a complete cycle of a DBD actuator in a well-characterized flow-field. The flow-field was a fully separated flat-plate boundary layer in a freestream pressure distribution designed to simulate that of a generic low-pressure turbine blade.   The primary diagnostic used in this study was high spatial-resolution, phase-locked PIV.   Two-dimensional velocity field measurements were acquired at each of thirty points along a complete cycle of the sinusoidal input wave of a DBD plasma actuator.
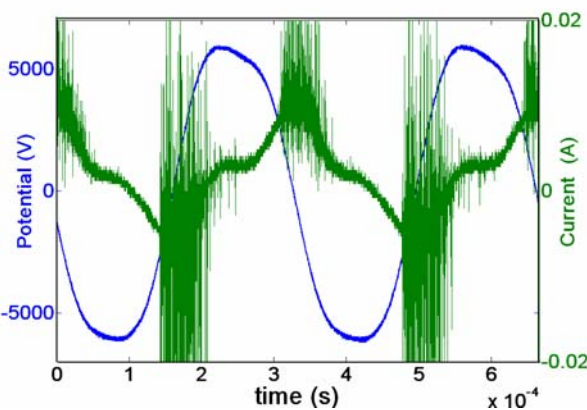

Figure 1 - Voltage and Current over DBD cycle

II.   Experimental Apparatus

This experiment used the same facility and experimental apparatus described in Boxx *et al.* (2006). The experimental apparatus is described in greater detail in that paper.

A. Plasma Actuator

The DBD flow-control actuator used in this study is shown in Figure 1. It consisted of two copper electrodes separated by a 1.56 *mm* thick layer of fiberglass laminate. The upper and lower electrodes are set in an asymmetric configuration with the upper electrode on the upstream side and the lower one on the downstream. Plasma generation occurs in the region where the electrodes run parallel to one another. This interface line is taken as the origin of the x-y coordinate system in this study.

The electrodes were driven with 3 *kHz* sine-wave A.C. signal. The signal was produced with an adjustable A.C. power supply (Compact Power - Titan Series™) connected to the primary coils of a pair of high-voltage step-up transformers (manufactured by Industrial Test Equipment Co.) which raised its voltage to 5-6 *kV (peak positive/negative)*.

Figure 2 - Schematic diagram of the dielectric barrier discharge flow-control actuator configuration

The voltage potential across the transformers was measured using a pair of 1000× voltage-attenuation probes (Tektronics Model P6015A). Current in the system was measured with a current coil (Pearson Model 4100). In order to correct for induction and capacitance inherent in the power-conditioning system, a baseline case (using a series of low-impedance pure resistors in place of the actuator) was also measured using the same instruments.

B. Low-Speed Wind Tunnel

The experiment was conducted in the low-speed wind-tunnel section of the Turbine Aero Thermal Basic Research Facility at the Air Force Research Laboratory. The facility has a rectangular test-section measuring $0.38 \times 0.25\ m$. Temperature of the flow through the tunnel was regulated and set to 26.6 deg C. (80 F) using a water-cooled chiller unit. Flow through the facility was seeded with propylene-glycol/water droplets (nominally 4 *μm* diameter) from a theatrical fog generator (Rosco Model 4500).

The actuator described above was mounted on a flat plate located in the test-section of the tunnel. A recess milled into the upper surface of the plate ensured the

Figure 3 - Low speed wind tunnel and PIV setup

actuator remained flush with the surface. The active (i.e. the plasma-generating) region of the actuator spanned only the center 95 *mm* of the plate in order to avoid wall-effects from the sides of the tunnel. A contoured block of polystyrene foam was mounted on the upper surface of the test section. The contour was designed to generate a pressure distribution approximating that of suction-side of a generic aft-loaded, low-pressure turbine blade. In order to keep flow attached over the contour a vacuum was applied to a 0.25" long slot which spans the width of the block
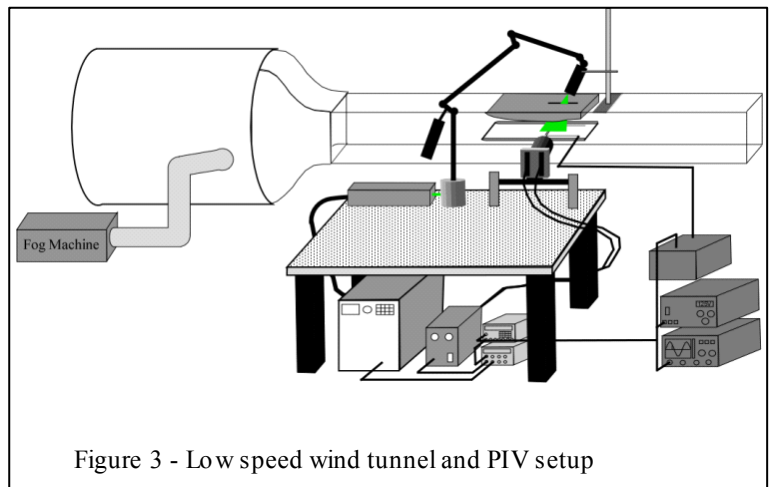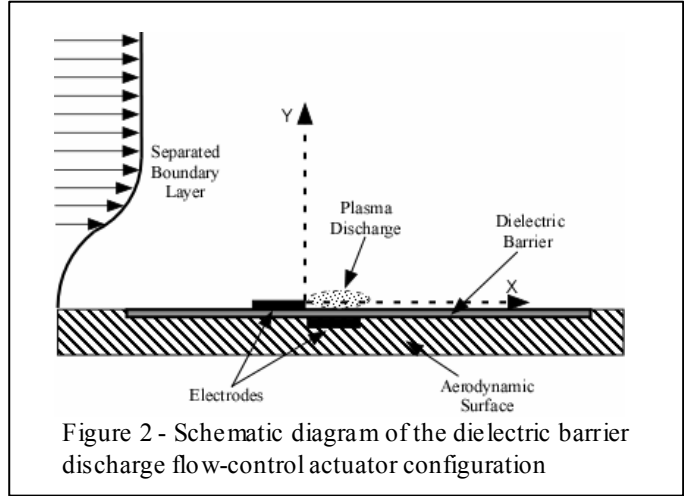
downstream of the throat of the contoured section. The vacuum was generated using a highly-throttled, 2HP commercial shop-vac system.

C. PIV System

The PIV system used a dual-head, frequency-doubled, flashlamp-pumped Nd:YAG laser (New Wave Solo-120) and an adjustable light-arm to deliver sheet-illumination to the test-section. Light scattered from propylene-glycol seeding droplets was imaged with a high-framerate, 1024×1024 pixel resolution CMOS camera (Photron-APX). The camera was triggered in a two-frame burst mode at a 10 Hz repetition rate to produce a frame-straddling PIV system. The camera was equipped with a 200 *mm* lens (Nikon, AF-Nikkor) operating at f/11. The field of view of the PIV system was 17.9×17.9 *mm*. Each pixel corresponds to 17.45 *μm* in physical space for approximately 1-to-1 imaging. The camera and lasers were synchronized using two pulse/delay-generator timing boxes (Stanford Research Systems DG-535 and Quantum Composers 9300 Series respectively). The images were processed with a commercially available adaptive window offset cross-correlation algorithm (Dantec FlowManager). The final window size was 32×32 pixels with 50% overlap for a final spatial resolution of ≈ 0.56 *mm* and vector placement every ≈ 0.28 *mm*. The data was then post-processed using in-house codes.

D. Boundary Conditions

The driver signal for the DBD actuator in this study was set to $3\,kHz$ and had a peak-to-peak potential difference of $12\,kV$. The local freestream velocity above the actuator location was $1.5\,m/s$ and $Tu = 4.6\%$ ($Tu = \sqrt{u'^2 + v'^2} / \sqrt{U^2 + V^2}$, where U and V are the local freestream velocity components in the x and y directions).

The static-pressure distribution along the test-section wall was measured at fourteen points using a pressure transducer (GE - Druck LPM 9481, 0.2" H_2O full-scale range). These pressures were used to compute the C_p distribution shown in the plot presented in Figure 4. C_p was defined as $C_p = (P_t - P_s)/(\frac{1}{2}\rho U^2)$, where U is the freestream velocity upstream of the actuator. As noted above, suction was applied to the contoured upper surface of the wind-tunnel test-section in order to prevent flow-separation there. The plot shown in Figure 4 also shows the C_p distribution for the case where no suction was applied to the upper surface. It can be seen from the similarity of the two profiles that although the applied suction resulted in an attached flow over the upper surface, it did not result in a substantial alteration of the freestream pressure characteristics. Comparing our measured C_p distribution to that of a generic low-pressure turbine airfoil, we determined that the contoured test-section produced and effective chord length of 0.35*m*, resulting in a simulated chord-Reynolds number of 23,500 for this study.

In order to better characterize the nature of the flow through the test-section, we also performed a series of wide-field PIV measurements using the system described above. The streamlines derived from these measurements are shown in Figure 5. Overlaid on these streamlines are the relative positions of the contoured upper section of the
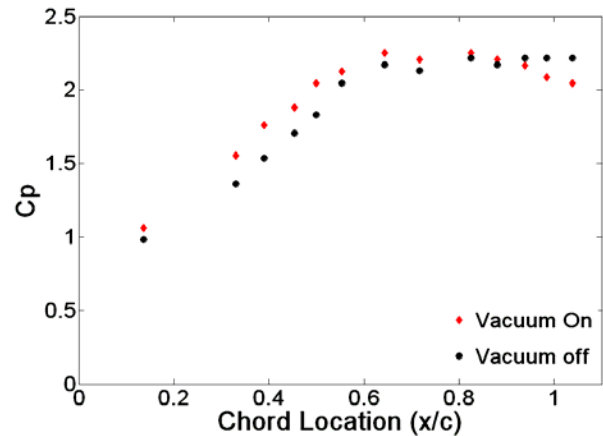

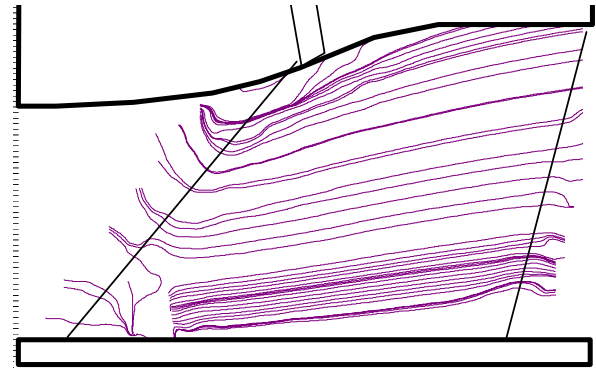Figure 4 – C_p distribution measured along test section.

Figure 5 – Streamlines of flow through the test-section in the vicinity of the actuator. The dashed lines show the approximate location laser-sheet cutoff, where particle-dropout was seen to result in a region of lower SNR.

wind-tunnel (including the slot where the vacuum was applied) and the outer bounds of the laser sheet illumination. We note that near the edges of the laser sheet, the signal-to-noise ratio of the measurements dropped off quickly, resulting in the misshapen streamlines shown there in the image.

It is clear from these streamlines that the suction applied to the contoured upper section of the tunnel induced a small but noticeable ($\approx 0.2m/s$) velocity in the vertical direction. Although this added vertical velocity was

4

undesirable it was necessary in order to maintain stability and uniformity in the test-section. The vertical velocity induced by the vacuum provided an additional challenge to flow-reattachment and thus allowing a more rigorous test of the capabilities of the flow-control actuator.
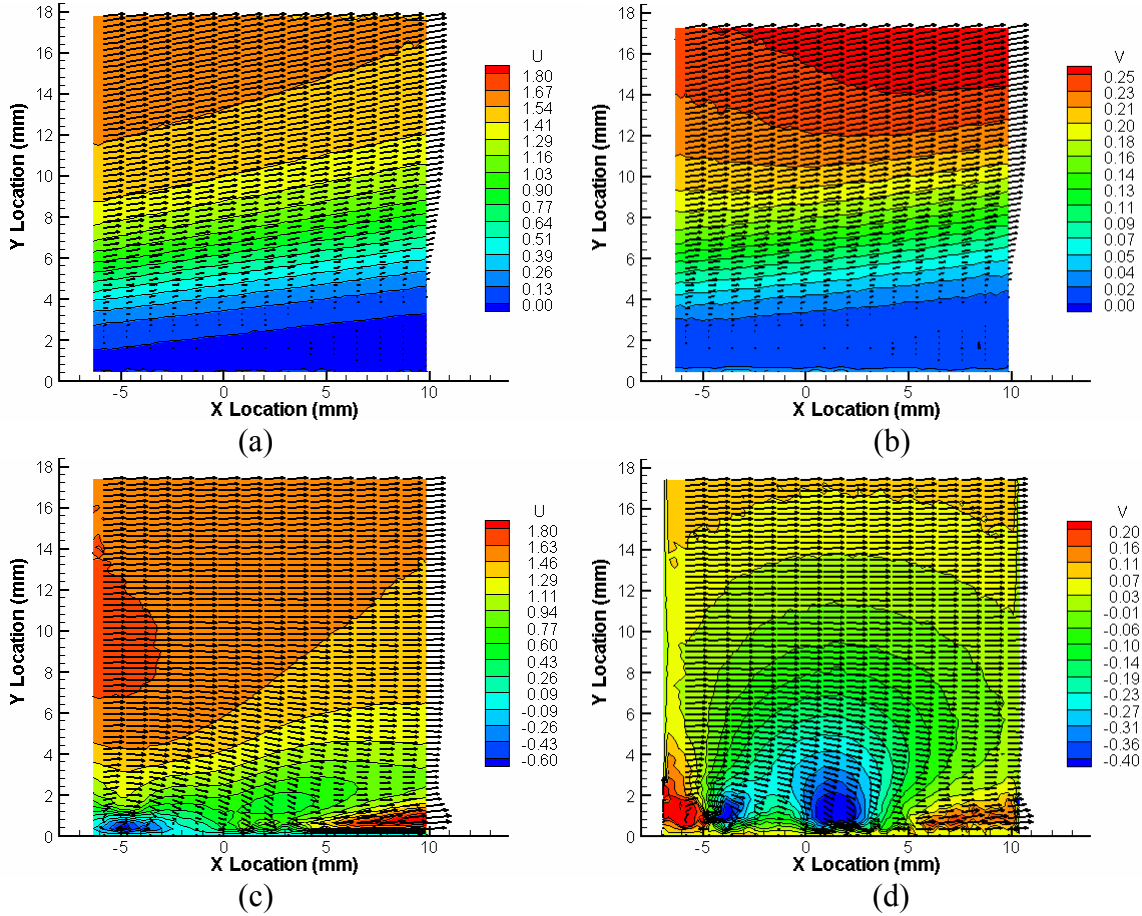
III.   Results and Discussion

Figure 6 - Representative velocity fields measured in the boundary layer. (a) and (b) show the U- and V-velocity components measured in the initially separated boundary layer respectively. (c) and (d) show this same for the actuated boundary layer. Units are in m/s.

A. Velocity Field Measurements

Figure 6 shows the measured velocity fields in the streamwise and normal directions for the initially separated boundary layer and a representative sample of the velocity fields for the actuated boundary layer. Before discussing the phase-dependent response of the boundary layer velocity field, it is instructive to examine the general response and behavior of the boundary layer when acted upon by the DBD actuator.

Figure 6a and 6b show the U- and V-components of velocity for the case of the un-actuated boundary layer. In this figure, the axes are referenced such that the origin corresponds to the center of the two electrodes on the actuator. Both the vectors and contours of U- velocity show that the boundary layer is fully separated in the un-actuated case. Although the separation begins upstream of the PIV window, it is straightforward to estimate its location to be ≈ 12 - 15*mm* upstream of the origin by tracing the lowest U-velocity contour to its intersection with the streamwise axis. The contours of V-velocity in Figure 6b illustrate the previously mentioned vacuum-induced V-velocity. Although previous studies have indicated that placing the actuator immediately upstream of the separation is most effective for preventing flow-separation over an airfoil we find that placing it in the stagnant near-wall fluid of an already separated boundary layer gives the clearest contrast in the PIV measurements and thus provides further insight into the nature of the actuator / boundary-layer interaction.

Comparing the measured velocity fields shown in Figure 6a and 6b with those in 6c and 6d the effect of the actuator is clear. The U-velocity contours show the actuator affects a re-attachment of the boundary layer downstream of its location. Consistent with previous research, we see a region of high (relative) velocity fluid jetting along the wall downstream of the actuator. Above this region exists an area of lower-velocity but still attached boundary layer flow. Upstream of the actuator however there is a standing separation bubble. Previous research in the present study (Boxx *et al.*, 2006) has shown that this separation bubble decreases both in strength and spatial magnitude with increasing voltage and/or power input to the actuator. In order to prevent unnecessary wear on the dielectric barrier material we decided against increasing the power input to the levels required to eliminate this separation bubble altogether.

The measured V-velocity field shown in Figure 6d indicates the extent to which the actuator influences the velocity normal to the aerodynamic surface. Figure 6d shows that the actuator counteracts the initial vertical vacuum-induced vertical velocity and induces a net downward velocity throughout most of the field of view. This downward velocity peaks immediately downstream the origin, i.e. near the interface of the actuator electrodes. This corresponds to the location of plasma generation by the actuator and the most intense concentration of E-field lines over the actuator. A secondary peak in the V-velocity field occurs approximately 4 *mm* upstream of the origin. Comparison of Figures 6c and 6d shows that this secondary peak in downward pointing (negative) V-velocity is in the region of the aforementioned upstream separation bubble. Figure 6d also shows an increased velocity in the vertical direction associated with the jetting region downstream of the actuator. It is not clear if this is the result of charged particles following the field lines of the actuator or if it's a thermal effect induced by heating caused by the plasma. The spatial extent of the actuators influence upon the vertical velocity field is significantly larger than that of its effect on the streamwise velocity.

B. Phase-localized measurement of U-velocity in the upper boundary-layer region
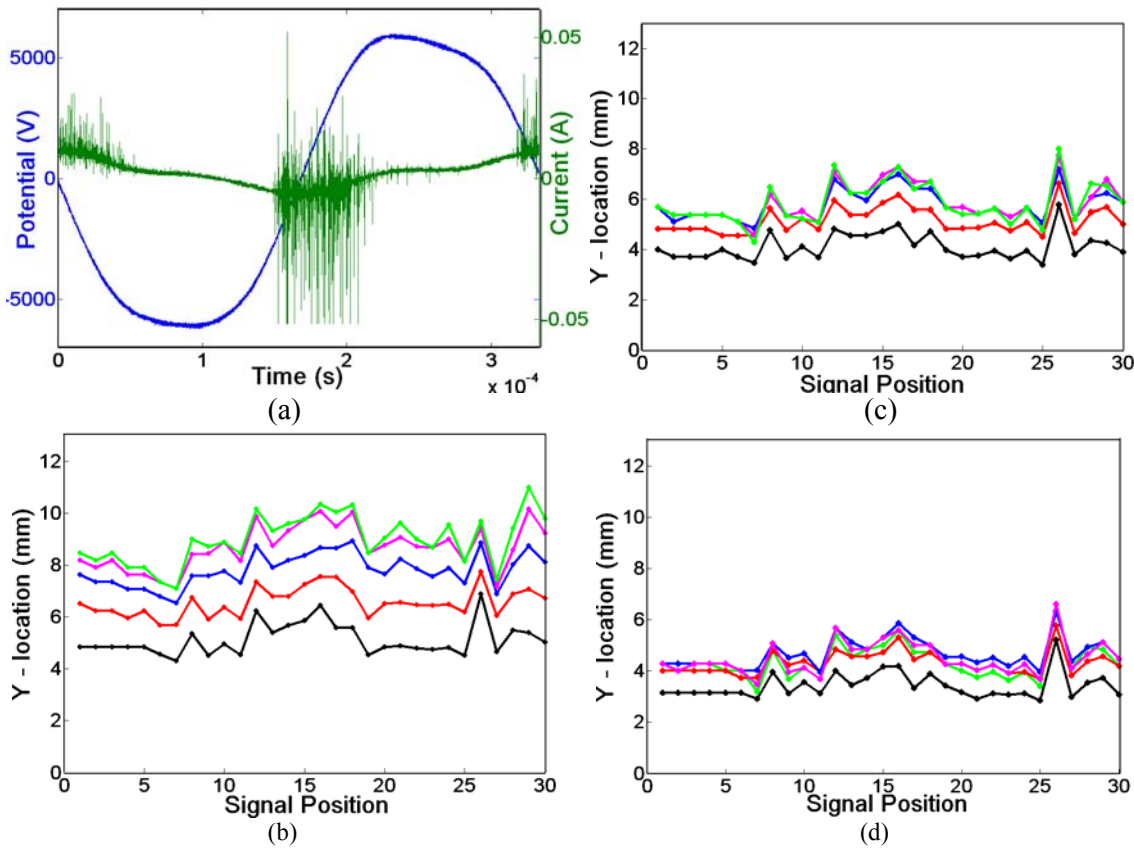

(a)

(b)

(c)

(d)

Figure 7 – Measured heights of U-velocity contours vs. the phase of the input signal to the actuator with increasing downstream distance. (a) Representative voltage and current trace measured to actuator (b) 90% peak U-velocity (c) 80% peak U-velocity (d) 70% peak U-velocity.
Legend – Black = 0mm, red = 2.7mm, blue = 5.4mm, magenta = 8.3mm, green = 9.9mm

Previous research has focused upon the effect of these actuators upon the C_P distribution and near-wall velocity field modification (Boxx *et al.*, 2006). The PIV data for each phase angle was threshholded to determine the 70, 80 and 90% freestream velocity contours. The height of each of these contours was then extracted from the data at several downstream locations and plotted against their corresponding phase-angles. These plots are shown above, in Figure 7. Comparing the height of the velocity contours to the corresponding phase angles of the input signal to the actuator reveals a subtle correlation. There is a considerable change in the U-component of velocity associated with upwards rising zero-cross of the actuator input signal. There is also a (much smaller) change in U-velocity associated with the downward falling zero-cross of the input voltage signal to the actuator. These phase-localized changes in the height of the U-velocity contours are most evident for the case of the 90% contour, shown in Figure 7b but can be seen in all three contours plotted in Figure 7. The reason for the observed changes in U-velocity component with phase-location becomes clear when comparing the data to measured current traces rather than the input voltage signal.

Figure 7a. shows a representative voltage and current trace for the actuator at the conditions examined in this study. Consistent with previous researcher observations, we note clusters of large (relative) magnitude spikes in the measured current signal associated with the upward rising and downward falling zero-cross of the input voltage signal. As noted in a previous section, researchers have linked these current spikes to the ignition and quenching of the plasma across the DBD actuator. As can be seen in Figure 7a, the current associated with these clustered spikes and be orders of magnitude greater than the current flowing during other phases of the cycle. The data shows that this increased current density changes the actuator effectiveness during the portion of the cycle where they occur. Figure 7 shows that the increased current density associated with the ignition and quenching events has a subtle, though observable influence on the upper reaches of the boundary layer and its coupling with the freestream flow.

The net effect of this phase-localized change in the U-velocity profile is negative. Rather than drawing high-velocity freestream fluid closer to the surface during the events, these current spikes have the opposite effect. The boundary-layer thickness increases during these events, suggesting that that these spikes inhibit the effective operation of the actuator. Increased thermal dissipation caused by increased current density may be the cause of the observed increase in boundary layer thickness.

It should be noted at this point that a limitation of the experimental apparatus may have biased the magnitude of the observed variation resulting in a lower magnitude change than would have otherwise been measured. This limitation is a result of the 110μs time-separation of the laser pulses in the PIV setup needed to resolve the relatively low-velocity flow. This corresponds to approximately one third the time-scale of the 3-*kHz* voltage driver signal to the actuator. As can be seen in Figure 8, the effect of taking a running average of a sine wave over one third of a cycle has the effect of reducing the magnitude of a signal by smoothing or blurring the data. As Figure 7 shows the flow responds to the forcing of the actuator at the frequency of the input signal there should be a smoothing effect associated with the 1/3rd cycle delta-t of the PIV measurement. Combining this with the localized clusters of current spikes the time-delay of the PIV system may result in a smaller magnitude difference in the measured velocity response.
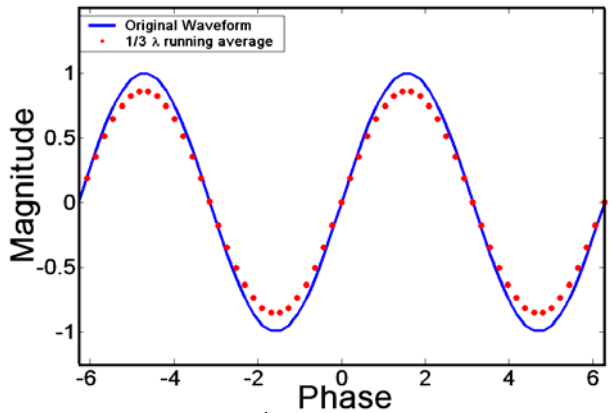

Figure 8 – Effect of 1/3rd cycle running average taken over over the period of a sine wave.

C. Phase-localized measurement of V-velocity field

Figure 9 shows the line-contours of V-velocity derived from representative points in the PIV measurements. The points used correspond to that shown in Figures 6c and 6d. It is clear from this figure that (unlike for the U-velocity field) the contours vary in two dimensions. The histograms of the V-component of velocity were compared over the entire field of view of the PIV system. This allowed for the slight two-dimensional variations of given V-velocity contours while still capturing the characteristics of the flow-field.

Figure 10 shows the histograms for the V-component of velocity for the initial, separated boundary layer as well as for several sequential phase-locations along the actuator input cycle. Figure 10 illustrates the differences in the V-velocity fields before and after the application of the actuator forcing. The initial histogram for that case is dual-peaked, with one peak at zero (corresponding to the stagnant fluid in the separation region) and a larger peak near 0.2 *m/s*. The histogram shows a uniformly positive V-velocity field for the unforced case. The histograms for the actuated case in Figure 10 are dual peaked. There is one peak at 0 *m/s* and a second peak between 0.04 - 0.08 *m/s*. Figure 9 shows the positive peak corresponds to fluid in the upper boundary layer and freestream flow. Although there is significant vertical velocity in the upward direction associated with the jetting downstream of the actuator the spatial extent over which this occurs in the PIV window is small and does not appear to have a major influence on the histogram profile. The measurement was limited by

Figure 9 – Contours of V-velocity in the actuated boundary layer.

the width of the PIV window and the V-component velocity associated with the jetting region will continue to grow with increasing distance downstream.

The histogram profile for the actuated boundary layer case indicates that V-velocity imparted by the actuator acts over a wide area of the PIV window. This can be seen by comparing it to the histogram profile of the un-forced case. The profile of the separated boundary layer cuts off sharply at zero velocity, the histogram profile for the actuated case drops off much more slowly.

Figure 11 shows the histograms of V-velocity for each of the thirty phase-angles in this study. The four plots that are shown each correspond to a quarter cycle of the input signal. In all cases the histogram has a dual-peak profile with a slowly decaying tail on the negative side. The magnitude of the histogram peaks while not identical do not vary significantly with the phase of the cycle. The rate of decay of the tails of the histogram show small variations.

Figure 10 – Histogram of V-velocity in the boundary layer. Solid black line corresponds to the histogram of the initial, separated boundary layer. The remaining curves represent samples of the actuated boundary layer V-velocity field at sequential phase angles.

CONCLUSIONS

Detailed experimental measurements of the global- and phase-dependent response of a separated boundary layer to the forcing of a dielectric-barrier discharge plasma flow control actuator were presented. The data showed a subtle phase-dependence in the U-component of velocity in the upper boundary layer to forcing by the actuator. This phase-dependence is linked to the clusters of current-spikes which occur during distinct portions of the a.c. discharge cycle and has the effect of increasing the boundary layer thickness. No similar phase-dependence was observed in the measured data for the V-component of velocity.
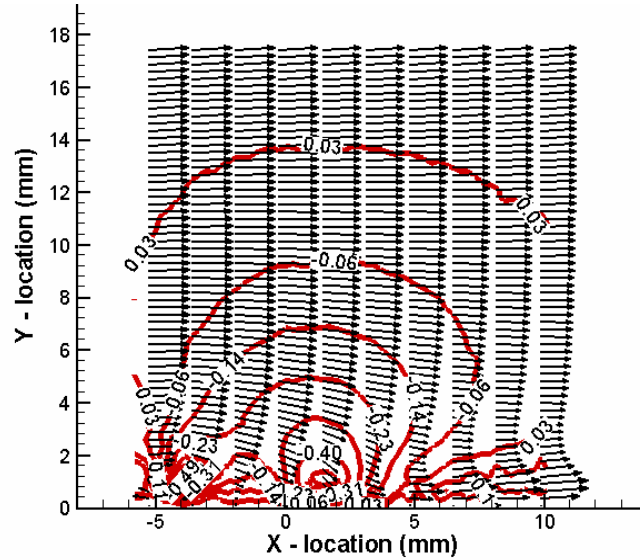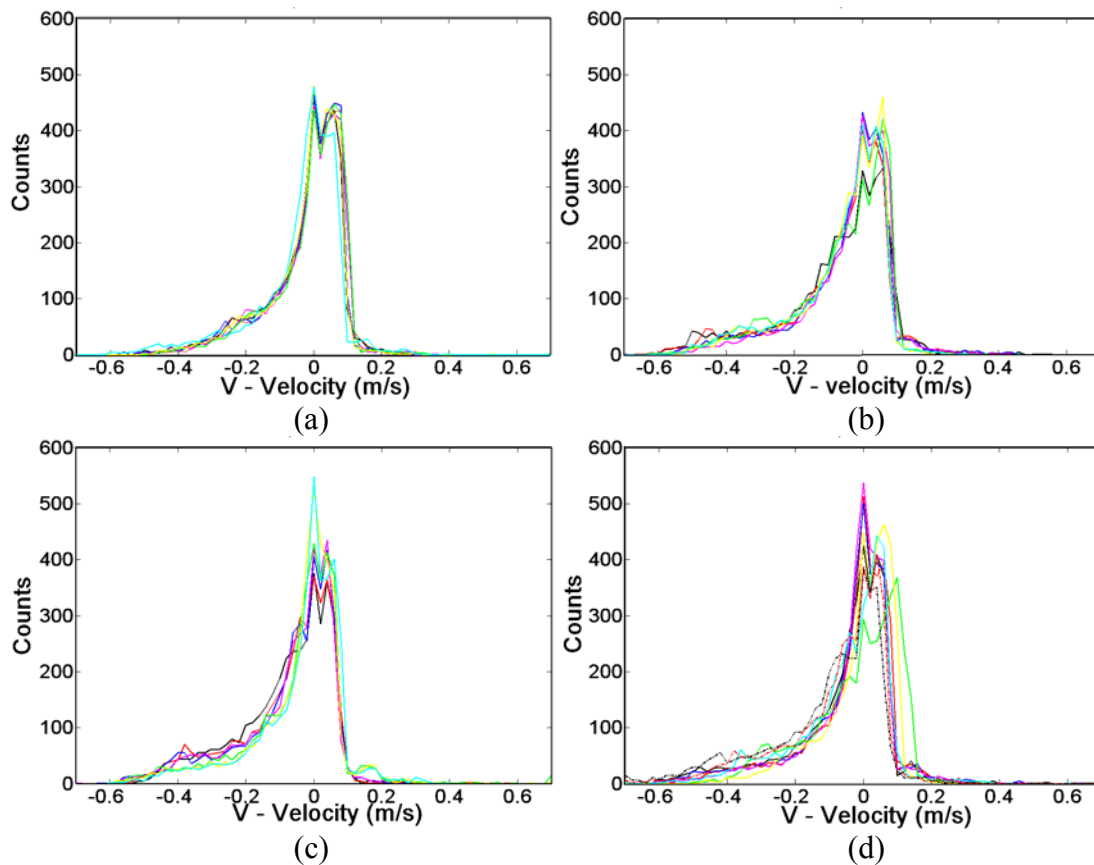
Figure 11 – Histograms of V-velocity measured in PIV window for each quarter of the actuator input cycle. a, b, c and d., correspond to the first, second, third and forth quarter of the voltage / current cycle shown in Figure 7a.

References

Corke, T.C., Cavalieri, D.A. "Controlled experiments on instabilities and transition to turbulence in supersonic boundary layers". AIAA 97-1817. 1997.

Enloe, C.L., McLaughlin, T.E., VanDyken, R.D., Kachner, D., Jumper, E.J., Corke, T.C. "Mechanisms and Responses of a Single Dielectric Barrier Plasma Actuator: Plasma Morphology", AIAA Journal, Vol. 43(3). 2004.

Huang, J., Corke, T.C., Thomas, F.O. "Plasma actuators for separation control of low pressure turbine blades", AIAA 2003-1024.

Hultgren, L.S., Ashpis, D.E. "Demonstration of separation delay with glow-discharge plasma actuators". 41st Aerospace Sciences Meeting and Exhibit, Reno NV. AIAA-2003-1025. 2003.

List, J., Byerley, A.R., McLaughlin, T.E., van Dyken, R.D. "Using a plasma actuator to control laminar separation on a linear cascade turbine blade". 41 Aerospace Sciences Meeting and Exhibit. Reno, NV. 2003.

McLaughlin, T.E., Munska, M.D., Vaeth, J.P., Dauwalter, T.E., Good, J.R., Siegel, S.G., "Plasma-based actuators for cylinder wake vortex control". AIAA 2004-2129. 2004.

Post, M. L., Corke, T.C. "Separation control on high angle of attack airfoil using plasma actuators". 41st Aerospace Sciences Meeting and Exhibit, Reno NV. AIAA 2003-1024. 2003.

Post, M.L., Corke, T.C. "Separation control using plasma actuators – Stationary and oscillating airfoils". AIAA 2004-0841. 2004.

Roth, J.R., Sherman, D.M, Wilkinson, S.P. "Boundary layer flow control with a one atmosphere uniform flow discharge surface plasma" . AIAA 98-0328. 1998.

Roth, J.R., Madhan, R.C.M, Yadav, M., Rahel, J., Wilkinson, S.P. "Flow field measurements of paraelectric, peristaltic, and combined plasma actuators based on the one atmosphere uniform glow discharge plasma (OAUGDP^{TM})" . 2004-845. 42nd AIAA Aerospace Sciences Meeting and Exhibit, Reno NV. 2004

Velkoff, H. R., "Investigation of the effects of electrostatic fields on heat transfer and boundary lasers", Ph.D. Dissertation. Ohio State University, 1962.